

Formation of longitudinal patterns and dimensionality crossover of nonlinear spin waves in ferromagnetic stripes

V. E. Demidov,¹ U.-F. Hansen,¹ O. Dzyapko,¹ N. Koulev,¹ S. O. Demokritov,¹ and A. N. Slavin²

¹*Institut für Angewandte Physik, Corrensstraße 2/4, 48149 Münster, Germany*

²*Department of Physics, Oakland University, Rochester, Michigan 48309, USA*

(Received 7 August 2006; published 29 September 2006)

Formation of stationary longitudinal amplitude patterns by propagating nonlinear spin waves has been discovered and studied experimentally by means of space-resolved Brillouin light scattering spectroscopy. The pattern formation is observed for spin waves propagating in narrow, longitudinally magnetized yttrium iron garnet stripes, characterized by attractive nonlinearity in both the longitudinal and transverse directions. A clear crossover of the effective dimensionality describing the propagation of spin waves in the stripe is observed with increase of the wave amplitude.

DOI: [10.1103/PhysRevB.74.092407](https://doi.org/10.1103/PhysRevB.74.092407)

PACS number(s): 75.30.Ds, 75.40.Gb

Pattern formation in nonlinear media of different physical nature has been attracting significant attention as one of the universal phenomena in nonlinear physics.¹ Recently, formation of spatially extended patterns has been intensively studied in optical media,^{2,3} as well as in Bose-Einstein condensates of ultracold gases.^{4,5}

Symmetry plays a decisive role in pattern formation. From this point of view ferromagnets are uniquely positioned, since an important inversion symmetry intrinsic for most physical systems is broken in a ferromagnet, because its magnetization is characterized by an axial vector. Thus, spin waves represent a superb object for nonlinear studies, allowing the observation of certain nonlinear effects, e.g., two-dimensional propagating wave bullets,^{6,7} that are difficult to observe experimentally in other nonlinear systems.⁸ Therefore experimental studies of pattern formation by spin waves can significantly contribute to this area. Many nonlinear wave phenomena that are common for all nonlinear systems, such as self-focusing, modulational instabilities, and temporal and spatial solitons, have been successfully observed and studied for spin waves (see, e.g., Refs. 9–15 and literature therein). At the same time, such an important nonlinear effect as the formation of spatially extended spin-wave patterns still remains insufficiently addressed. Several theoretical publications^{16,17} predicting formation of interesting patterns in spin-wave systems have not been supported by appropriate experimental studies up to now.

In this Brief Report we report on the observation and experimental study of stationary patterns that have no analog in other nonlinear media. The observed longitudinal patterns result from strong nonlinear interaction between the wave modes created in the sample due to transverse confinement. We show that a special combination of nonlinear and dispersion properties of the waves under consideration, which is hard to realize experimentally in other nonlinear systems, is necessary for existence of these patterns. We also present a theoretical model describing them.

The spatiotemporal evolution of a spin wave with frequency ω and wave vector k_0 propagating in a two-dimensional medium along the direction z is described by the (2+1)-dimensional nonlinear Schrödinger equation¹⁸ (NLSE)

$$i \left(\frac{\partial \varphi}{\partial t} + V_g \frac{\partial \varphi}{\partial z} \right) + \frac{D}{2} \frac{\partial^2 \varphi}{\partial z^2} + S \frac{\partial^2 \varphi}{\partial y^2} - N |\varphi|^2 \varphi = -i \omega_r \varphi, \quad (1)$$

where $\varphi(y, z, t)$ is the wave amplitude, $V_g = \partial \omega / \partial k_z|_{k_0}$ is the group velocity, $D = \partial^2 \omega / \partial k_z^2|_{k_0}$ is the dispersion coefficient, $S = \partial^2 \omega / \partial k_y^2|_{k_0}$ is the diffraction coefficient, $N = \partial \omega / \partial |\varphi|^2|_{k_0}$ is the nonlinear coefficient, and ω_r is the relaxation frequency. The early analysis of Eq. (1) performed in Ref. 19 has shown that, in the particular case of waves with $SN < 0$ and $DN < 0$, the uniform distribution of wave amplitudes is unstable in both the longitudinal and the transverse directions. The transverse instability leading to the spatial self-focusing effect has been experimentally observed for both stationary beams and wave packets.^{6,7,9,10}

However, in a medium confined in the y direction (i.e., in a stripe) transverse instability is strongly suppressed, if the width of a stripe is smaller than the instability half wavelength.²⁰

$$W < \frac{\pi}{k_y} = \frac{\pi}{|\varphi|} \sqrt{\frac{S}{N}}. \quad (2)$$

Rewriting the inequality (2) for light waves in a medium with the Kerr nonlinearity, one gets $W < \lambda / 2 \sqrt{n / \delta n}$, where λ is the wavelength, n is the refraction index of the medium, and δn is its nonlinear change. Taking the value δn , typical for optical systems,²¹ $\delta n / n \sim 10^{-4}$, one gets $W < 30 \mu\text{m}$. On the contrary, for spin waves propagating in yttrium iron garnet (YIG) films with a thickness of several micrometers the above condition (2) is satisfied, if the width $W < 1.5\text{--}2 \text{ mm}$. A magnetic stripe with such a width can be easily prepared and investigated by means of standard experimental methods. This allows one to study nonlinear spin-wave propagation in a unique case where the attractive nonlinearity acts in the transverse direction, but the self-focusing effects are suppressed.

In this work we studied the propagation of intense monochromatic spin waves in longitudinally magnetized YIG stripes with a thickness of $5.1 \mu\text{m}$, widths W of 1.1 and 1.6 mm, and length of 30 mm. The realized geometry corresponds to the so-called backward volume magnetostatic spin waves (BVMSWs), satisfying the above conditions $SN < 0$

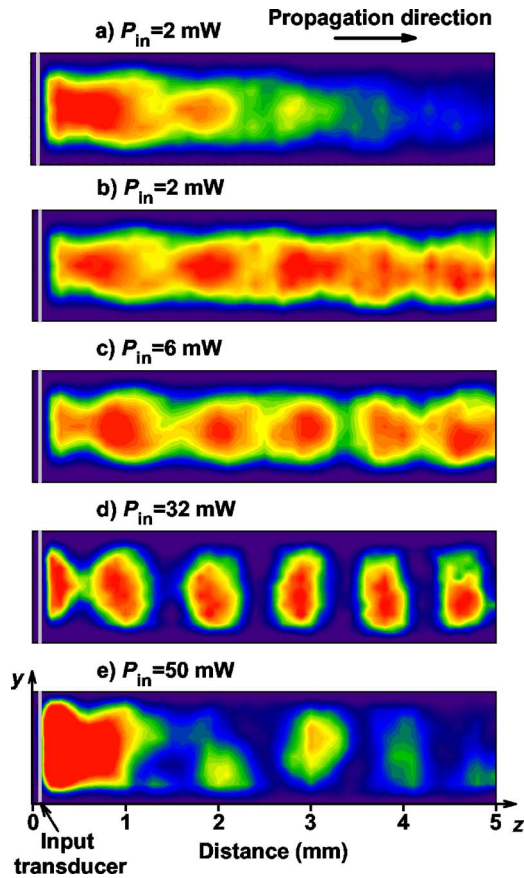


FIG. 1. (Color online) Two-dimensional maps of spin-wave amplitude measured by BLS at different values of the microwave power P_{in} supplied to the input transducer. The scanned area has dimensions of $1.2 \times 5 \text{ mm}^2$. $H_0 = 1420 \text{ Oe}$, $\omega/2\pi = 5.98 \text{ GHz}$.

and $DN < 0$. The waves were excited by one or two $25\text{-}\mu\text{m}$ -wide and 2-mm -long microstrip transducers separated by 7.8 mm and placed perpendicularly to the stripe axis. To analyze spatial distributions of the spin-wave amplitude, the space-resolved Brillouin light scattering (BLS) technique in the forward scattering geometry²² was used. This method allows one to measure two-dimensional maps of the spin-wave amplitude $|\varphi(y, z)|$, with a spatial resolution down to $10 \mu\text{m}$.

Figure 1 demonstrates the development of spin-wave amplitude maps in the stripe with $W = 1.1 \text{ mm}$, as the microwave power P_{in} supplied to the input transducer increases. The magnetic field and the excitation frequency were $H_0 = 1420 \text{ Oe}$ and $\omega/2\pi = 5.98 \text{ GHz}$. The scanned area has dimension of 1.2 and 5 mm along the transverse and the longitudinal directions, respectively.

For a relatively small input microwave power $P_{in} = 2 \text{ mW}$ [see Fig. 1(a)] spin waves propagate in the form of a well-defined beam showing a monotonic exponential decay along the propagation coordinate, $|\varphi| \sim e^{-z/\xi}$. Although the decay is relatively slow ($\xi = 5.3 \text{ mm}$), for the above presentation it conceals the fine structure of the beam. Therefore for the sake of clearness the original data in Figs. 1(b)–1(e) are multiplied by $e^{z/\xi}$. Figures 1(a) and 1(b), presenting the same data without and with the compensation, illustrate the advan-

tage of the latter presentation. As seen from Fig. 1(b), the amplitude of the beam is almost uniform along the propagation direction, whereas it decreases toward the edges of the stripe due to strong pinning of the magnetic precession at the lateral edges.²³ Implying complete pinning, the transverse profile of the mode can be described²⁴ as

$$A(y) = \sin\left(\frac{p\pi}{W}y\right), \quad (3)$$

where $p = 1, 2, 3, \dots$ is the transverse quantization number. In experiment several transverse modes can be excited simultaneously. However, since the exciting microwave field is practically uniform over the stripe, it can efficiently excite only the odd modes with $p = 1, 3, 5$ with efficiency proportional to $1/p^2$.²⁵

In the case of linear propagation, the spin-wave beam is mainly constituted by the mode with $p = 1$. As the excitation power is increased [see Fig. 1(c)], a modulation of the beam-width becomes visible, which is associated with the growth of the amplitude of the mode with $p = 3$ with respect to that of the basic mode with $p = 1$. This is connected with energy transfer from the intense lowest transverse mode to the higher mode due to the nonlinear interaction between them. Two modes have different longitudinal phase velocities; therefore their interference leads to the appearance of a periodic spatial structure. The period of this structure can be approximately evaluated as $\lambda = W(H_0/4\pi M_s)$, if the dispersion of the spin waves is neglected. Here M_s is the saturation magnetization of YIG, $4\pi M_s = 1750 \text{ G}$.

With further increase of the input power the periodic structure becomes more pronounced and, at a certain value of the power, transforms into a sequence of strongly localized amplitude maxima [see Fig. 1(d)]. A clear longitudinal pattern is created, consisting of several well-defined periodically situated areas where the spin-wave amplitude is nearly uniform in the transverse direction. As the numerical analysis shows, such a structure cannot result from linear interference between the transverse modes. Instead, it is a stable, phase-correlated bound state of many transverse modes strongly interacting with each other due to the nonlinear coupling, similar to the spatial-soliton states in continuous magnetic films.¹⁰

The pattern was found to exist in a certain range of the input power only. As seen from Fig. 1(e), a further increase of P_{in} leads to an abrupt breaking of the pattern.

Figure 1 also demonstrates a crossover with respect to the effective dimensionality of the spin-wave propagation in the stripe. In fact, in the linear case a well-defined transverse spin-wave quantization similar to that found in microstripes²⁶ is observed. Transverse modes with different quantization numbers p are independent of each other and the wave propagation is described as quasi-one-dimensional as illustrated by Fig. 1(b). With increasing input power [see Fig. 1(c)] an intensive nonlinear interaction between the transverse modes starts and the wave propagation demonstrates a two-dimensional pattern, in which the width of the beam is significantly modulated. With further growth of the spin-wave amplitude the dimensionality crossover occurs in

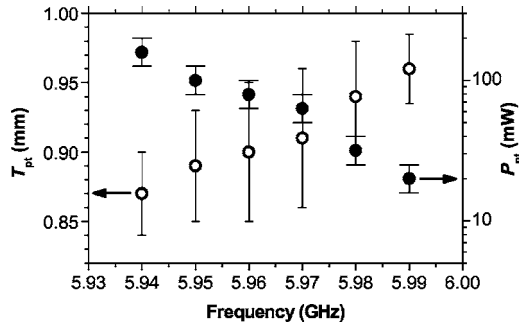


FIG. 2. Dependences of the power at which the pattern forms (solid circles) and the pattern period (open circles) on the excitation frequency. $H_0=1420$ Oe.

the opposite direction: quasi-one-dimensional spatial patterns with a constant width are formed [see Fig. 1(d)]. The above scenario is similar to that for the nonlinear soliton eigenmodes recently observed in active magnetic rings:²⁷ the symmetry of the stable nonlinear soliton mode differs dramatically from the symmetry of the linear eigenmodes in the system.

The formation of a stationary longitudinal pattern has been also observed in a ferromagnetic stripe with a width of 1.6 mm. For the same values of the frequency and the applied field the pattern period is increased by approximately 55% with respect to that in the stripe with a width of 1.1 mm. This fact clearly indicates the important role of the transverse modes in the pattern formation process. However, confirming the results of the above discussion of the inequality (2), in the wider stripe the pattern has an essentially two-dimensional character. Therefore, for a detailed study of the patterns the stripe with a width of 1.1 mm was used. In particular, we studied the properties of the pattern as a function of the wave vector of the wave. For this the static magnetic field was fixed at $H_0=1420$ Oe and the excitation frequency was decreased from the upper spin-wave cutoff frequency, which is equal to 6.00 GHz for the given field. The measured dependence of the threshold value of the input power P_{pt} at which the pattern formation starts on the input frequency is shown in Fig. 2 by solid circles. Since BVMSWs possess a negative group velocity, decrease of the frequency corresponds to increasing wave vectors. As seen from the figure, at frequencies near the cutoff frequency (small wave vectors), the pattern formation starts at relatively low powers below 20 mW. As the wave frequency decreases (wave vector increases), the threshold power P_{pt} rises exponentially and reaches values of more than 100 mW for a frequency offset of 60 MHz. The spatial period of the pattern, T_{pt} , was also found to be dependent on the excitation frequency as shown in Fig. 2 by open circles. However, the variation of T_{pt} over the studied frequency range does not exceed 10%.

The observed weak dependence of the pattern period on the frequency is not obvious, since the above changes of the spin-wave frequency correspond to drastic changes of the wave vector in the linear case. In order to measure the actual wave vectors of the nonlinear waves forming the patterns, a standing spin wave has been created in the sample by sending an additional probing, small-amplitude spin wave of the

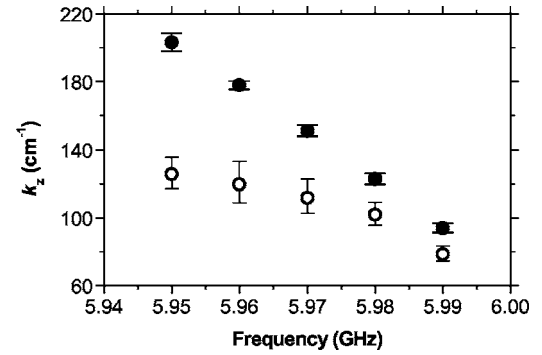


FIG. 3. Longitudinal wave vectors corresponding to different excitation frequencies for the case of linear propagation regime (solid circles) and for the power corresponding to the threshold of pattern formation (open circles). $H_0=1420$ Oe.

same frequency in the opposite direction using the second transducer. The data obtained in such a way are summarized in Fig. 3 where solid circles show spin-wave wave vectors k_z for relatively small input power of 2 mW, whereas open circles illustrate the same dependence for values of the input power just below the threshold of the pattern formation. A clear nonlinear negative shift of the spin-wave spectrum for high excitation power, manifesting itself as a significant shift of the carrier wavevector at a given frequency, is seen in the figure. Using the approximate value of the nonlinear coefficient, calculated for the spin-wave spectrum of a continuous film $N/2\pi=23$ GHz/rad², and the measured nonlinear shift, one obtains the maximum precession angle of the spin wave, at which the pattern formation starts, $\varphi=0.04$ rad= 2° . This value is of the same order of magnitude as the threshold of the soliton formation in continuous magnetic films.²²

As mentioned above, the period of the observed longitudinal pattern only slightly depends on the spin-wave wave vector. Instead, a significant change of the period was observed if the field H_0 was varied. Since the variation of H_0 results in a strong shift of the cutoff frequency, the excitation frequency for every field was fixed at a value of 20 MHz below the cutoff frequency. Figure 4 shows the experimental dependence of the pattern period T_{pt} as a function of the

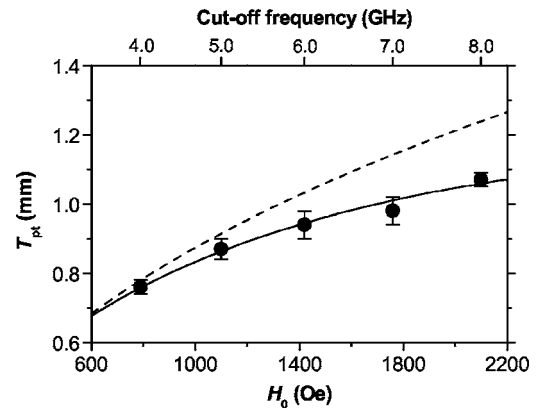


FIG. 4. Period of the longitudinal pattern as a function of the amplitude of the static magnetic field. Lines show the result of the numerical calculation as described in the text.

field. For the given range of H_0 the cutoff frequency grows from 4.00 GHz (790 Oe) to 8.00 GHz (2090 Oe) as is also shown in the figure. As seen in Fig. 4, with increasing magnetic field the spatial period of the pattern is approximately proportional to the field and increases from 0.76 to 1.11 mm. The field dependence of the pattern period has been calculated numerically using the spin-wave dispersion relation²⁸ and the mode profile law (3) corresponding to complete pinning. The result is shown in Fig. 4 by the dashed line. The solid line represents the result of calculation taking into account the exact pinning conditions at the edges of the stripe derived in Ref. 23 and using the pinning strength as a fit parameter. As seen in the figure, the agreement between the experiment and the calculation is convincing.

In conclusion, formation of longitudinal spin-wave patterns has been observed and studied. The period of the

formed pattern is proportional to the width of the ferromagnetic stripe, demonstrates monotonic dependence on the applied magnetic field, and is only weakly dependent on the wave vector of the wave. The patterns were found to be formed in a well-defined interval of the input microwave power and result from the nonlinear interaction of different transverse spin-wave modes of a ferromagnetic stripe. A simple model describes the dependence of the pattern period on the external field, stripe width, and the excitation frequency.

Financial support by the Deutsche Forschungsgemeinschaft, by the U.S. Army Research Office under the MURI Grant No. W911NF-04-1-0247 and ARO Grant No. W911NF-04-1-0299, and by the Oakland University Foundation is gratefully acknowledged.

-
- ¹M. Cross and P. Hohenberg, *Rev. Mod. Phys.* **65**, 851 (1993).
²F. Arecchi, S. Boccaletti, and P. Ramazza, *Phys. Rep.* **318**, 1 (1999).
³C. Denz, P. Jander, M. Schwab, O. Sandfuchs, M. Belic, and F. Kaiser, *Ann. Phys.* **13**, 391 (2004).
⁴K. Kasamatsu and M. Tsubota, *Phys. Rev. Lett.* **93**, 100402 (2004).
⁵K. Staliunas, S. Longhi, and G. J. de Valcarcel, *Phys. Rev. A* **70**, 011601(R) (2004).
⁶M. Bauer, O. Büttner, S. O. Demokritov, B. Hillebrands, V. Grimalsky, Y. Rapoport, and A. Slavin, *Phys. Rev. Lett.* **81**, 3769 (1998).
⁷O. Büttner, M. Bauer, S. O. Demokritov, B. Hillebrands, M. P. Kostylev, B. A. Kalinikos, and A. Slavin, *Phys. Rev. Lett.* **82**, 4320 (1999).
⁸X. Liu, K. Beckwitt, and F. Wise, *Phys. Rev. Lett.* **85**, 1871 (2000).
⁹J. W. Boyle, S. A. Nikitov, A. D. Boardman, J. G. Booth, and K. Booth, *Phys. Rev. B* **53**, 12173 (1996).
¹⁰M. Bauer, C. Mathieu, S. O. Demokritov, B. Hillebrands, P. A. Kolodin, S. Sure, H. Dötsch, V. Grimalsky, Y. Rapoport, and A. Slavin, *Phys. Rev. B* **56**, R8483 (1997).
¹¹M. Scott, B. Kalinikos, and C. Patton, *J. Appl. Phys.* **94**, 5877 (2003).
¹²M. Wu, B. A. Kalinikos, and C. E. Patton, *Phys. Rev. Lett.* **93**, 157207 (2004).
¹³B. A. Kalinikos, M. M. Scott, and C. E. Patton, *Phys. Rev. Lett.* **84**, 4697 (2000).
¹⁴A. N. Slavin and H. Benner, *Phys. Rev. B* **67**, 174421 (2003).
¹⁵M. Wu, M. A. Kraemer, M. M. Scott, C. E. Patton, and B. A. Kalinikos, *Phys. Rev. B* **70**, 054402 (2004).
¹⁶F.-J. Elmer, *Phys. Rev. Lett.* **70**, 2028 (1993).
¹⁷F.-J. Elmer, *Phys. Rev. B* **53**, 14323 (1996).
¹⁸A. Zvezdin and A. Popkov, *Sov. Phys. JETP* **57**, 350 (1983).
¹⁹M. J. Lighthill, *J. Inst. Math. Appl.* **1**, 269 (1965).
²⁰*Wave Turbulence Under Parametric Excitation*, edited by V. L'vov (Springer, Berlin, 1994).
²¹*Optical Solitons*, edited by K. Porsezian and V. C. Kuriakose (Springer, Berlin, 2003).
²²S. O. Demokritov, B. Hillebrands, and A. N. Slavin, *Phys. Rep.* **348**, 442 (2001).
²³K. Y. Guslienko, S. O. Demokritov, B. Hillebrands, and A. N. Slavin, *Phys. Rev. B* **66**, 132402 (2002).
²⁴T. O. Keeffe and R. Patterson, *J. Appl. Phys.* **49**, 4886 (1978).
²⁵S. Bajpai, *J. Appl. Phys.* **58**, 910 (1985).
²⁶C. Mathieu, J. Jorzick, A. Frank, S. O. Demokritov, A. N. Slavin, B. Hillebrands, B. Bartenlian, C. Chappert, D. Decanini, F. Rousseaux, and E. Cambriil, *Phys. Rev. Lett.* **81**, 3968 (1998).
²⁷S. Demokritov, A. Serga, V. Demidov, B. Hillebrands, M. Kostylev, and B. Kalinikos, *Nature (London)* **426**, 159 (2003).
²⁸R. W. Damon and J. R. Eshbach, *J. Phys. Chem. Solids* **19**, 308 (1961).